

# High-energy magnon dispersion in the half-filled Hubbard model: A comparison with $\text{La}_2\text{CuO}_4$

Pinaki Sengupta, Richard T. Scalettar and Rajiv R. P. Singh  
*Department of Physics, University of California, Davis, CA 95616*  
 (November 12, 2018)

We use quantum Monte Carlo methods and single-mode approximation to study the magnon dispersion in the 2D half-filled Hubbard and phonon-coupled Heisenberg models. We find that in the Hubbard model with  $U/t < 8$ , high-energy magnon dispersion is similar to those observed in inelastic neutron scattering experiments in  $\text{La}_2\text{CuO}_4$ . On the other hand, our studies of a 2D Heisenberg model coupled to dynamic optical bond phonons, fails to reproduce the experimental dispersion. These results can be interpreted as evidence for intermediate  $U/t$  and charge fluctuations in the cuprate materials.

PACS: 75.40.Gb, 75.40.Mg, 75.10.Jm, 75.30.Ds

While there is still no consensus on the microscopic origin of superconductivity in high-temperature copper oxide superconductors, it is widely believed that magnetic fluctuations play an important role. This has led to extensive studies of magnetic fluctuations in the parent compounds of these materials, such as  $\text{La}_2\text{CuO}_4$ . The low-energy long-wavelength properties of these layered compounds are well described by the non-linear sigma model and the renormalized classical theory<sup>1</sup>. However, short wavelength or high energy spin-fluctuations may also be relevant to superconductivity, which only sets in after long-range antiferromagnetic order is lost. The description of these excitations has raised many questions. Are there well-defined magnons at short wavelengths? Is there significant spectral weight in multimagnon excitations? Do the spinons present a better description of short-wavelength excitations? Is there a coexistence of spinons and magnons? The most quantitative theoretical studies have been done for the nearest-neighbor Heisenberg model, where one finds magnons throughout the Brillouin Zone, with significantly reduced spectral weight along the antiferromagnetic zone boundary<sup>2,3</sup>.

On the experimental side, Raman scattering has long provided evidence for anomalous short-wavelength spin fluctuations<sup>4</sup>. The line-shape of the two-magnon Raman spectra has not been adequately explained. Similar results are inferred from optical absorption spectra<sup>5</sup>. Understanding these spectra is complicated by the fact that light couples directly to the charge degrees of freedom and thus their understanding within a spin-only picture requires many assumptions<sup>6</sup>. In contrast, neutron scattering provides a direct probe of the spin excitations<sup>7,8</sup>. Recently, the high energy magnon dispersion has been measured in  $\text{La}_2\text{CuO}_4$  by inelastic neutron scattering. One finds magnon dispersion at short wavelengths, with  $(\pi/2, \pi/2)$  magnon energy about 13% lower than that at  $(\pi, 0)$ <sup>9</sup>. This is in contrast to results for the nearest-neighbor Heisenberg model, where one finds the magnon energy at  $(\pi, 0)$  to be 7–10% lower than at  $(\pi/2, \pi/2)$ <sup>2,3</sup>. The latter results have also been seen experimentally in the materials  $\text{Cu}(\text{DCOO})_2 \cdot 4\text{D}_2\text{O}$ <sup>10</sup> and  $\text{Sr}_2\text{Cu}_3\text{O}_4\text{Cl}_2$ <sup>11</sup>.

Explanation for the anomalous dispersion in  $\text{La}_2\text{CuO}_4$  has evoked considerable interest. Adding a second neighbor antiferromagnetic exchange takes the spectra in the opposite direction, ruling out the simplest possibility. One mechanism that has been suggested is ring exchange of four electrons in a plaquette<sup>9</sup>. Such a term can be directly obtained from the Hubbard model<sup>12</sup> and was first proposed for the high- $T_c$  materials to explain the Raman spectra more than a decade ago<sup>13</sup>. One interesting aspect of the ring-exchange term is that, when treated fully, it does not change the spin-wave dispersion within linear spin-wave theory. Thus its effect on the dispersion is a purely quantum effect. Recent numerical studies have focused on whether such a term can explain the experimental dispersion without destabilizing Néel order<sup>14</sup>.

In a recent paper, Peres and Araújo<sup>15</sup> have studied the 2D Hubbard model using mean-field theory and obtained a dispersion relation similar to that observed in  $\text{La}_2\text{CuO}_4$  for an intermediate value of the on-site interaction parameter,  $U/t = 6$ , indicating that charge fluctuations – ignored in the Heisenberg model – need to be taken into account to explain the properties of this material. Given the inherently approximate nature of the mean-field theory, it is important to confirm and extend this result using independent approaches. We have used the determinant quantum Monte Carlo (det QMC) method and single mode approximation (SMA) to study the magnon dispersion in the 2D Hubbard model at half-filling. The det QMC method has been extensively used to study the ground state properties of the 2D Hubbard model at half-filling where the fermion sign problem can be avoided. We have studied the magnon dispersion along the magnetic zone boundary as a function of the on-site interaction parameter,  $U/t$ . We find that with decreasing  $U$ , the zone-boundary dispersion changes sign and for  $U/t < 8$  it becomes similar to those observed in  $\text{La}_2\text{CuO}_4$ .

Coupling to phonons is another potential source of anomalous dispersion in the cuprates, because of the rather high magnon energies. We have used the stochastic series expansion QMC to study a Heisenberg model coupled to optical bond phonons. We find that such a

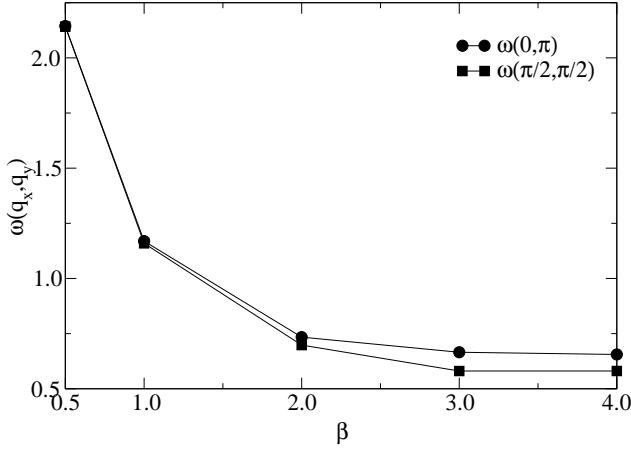


FIG. 1. Convergence of magnon energy to the ground state value as a function of the inverse temperature for a lattice of size  $N=8 \times 8$  at  $U=6.0$ . Error bars are smaller than symbol sizes.

model fails to reproduce the experimental spectra. While suggestive, this, however, does not rule out the possibility that a more realistic treatment of the spin-phonon couplings can mimic the experimental results.

The Hubbard model in two dimensions is given by the Hamiltonian

$$H = -t \sum_{\langle \mathbf{i}, \mathbf{j} \rangle \sigma} (c_{\mathbf{i}, \sigma}^\dagger c_{\mathbf{j}, \sigma} + c_{\mathbf{j}, \sigma}^\dagger c_{\mathbf{i}, \sigma}) + U \sum_{\mathbf{i}} (n_{\mathbf{i}, \uparrow} - \frac{1}{2})(n_{\mathbf{i}, \downarrow} - \frac{1}{2}) + \mu \sum_{\mathbf{i}} n_{\mathbf{i}}, \quad (1)$$

where  $c_{\mathbf{i}, \sigma}^\dagger$  ( $c_{\mathbf{i}, \sigma}$ ) creates (annihilates) an electron with spin  $\sigma$  at lattice site  $\mathbf{i}$ . The kinetic energy term includes a sum over nearest neighbors  $\langle \mathbf{i}, \mathbf{j} \rangle$  and  $t$  is the hopping integral between adjacent sites.  $U$  is the on-site interaction, and  $\mu$  is the chemical potential. We shall be dealing solely with the half-filled band, i.e.,  $\langle n_{\mathbf{i}, \uparrow} + n_{\mathbf{i}, \downarrow} \rangle = 1$ . With the interaction term written in a particle-hole symmetric form as above, the half-filled band corresponds to setting  $\mu = 0$ . Henceforth we set  $t = 1$  and express the interaction parameter  $U$  in units of  $t$ .

In the limit of large  $U$ , the Hubbard model at half-filling maps on to the Heisenberg model with exchange parameter  $J = 4t^2/U$ . The Heisenberg model in 2D is given by the Hamiltonian

$$H = J \sum_{\mathbf{i}, \mathbf{j}} \mathbf{S}_{\mathbf{i}} \cdot \mathbf{S}_{\mathbf{j}} \quad (2)$$

The spin operators are related to the electron creation and annihilation operators by the relation

$$\mathbf{S}_{\mathbf{i}} = \frac{1}{2} c_{\mathbf{i}, \sigma}^\dagger \vec{\tau}_{\sigma, \sigma'} c_{\mathbf{i}, \sigma}$$

where  $\vec{\tau}$  are the Pauli matrices.

The det QMC<sup>16</sup> used to study the 2D Hubbard model is a finite temperature method that is based on discretizing the imaginary time  $\beta = L\Delta\tau$  and employing Trotter approximation to decompose the full imaginary-time evolution. This approach treats the electron-electron interactions exactly and at half-filling, where we focus in this work, is able to produce results with small statistical fluctuations. Ground state expectation values are obtained using sufficiently large values of  $\beta$ . Like most other numerical approaches, the technique is limited to finite-size lattices and we have been able to study primarily two different lattice sizes,  $N=6 \times 6$  and  $N=8 \times 8$ . While this is not sufficient to do a complete finite-size scaling analysis to obtain thermodynamic expectation values, previous studies have shown that a lattice of size  $N=8 \times 8$  is large enough to give reasonably good estimates of the thermodynamic limit, especially when measuring quantities away from the antiferromagnetic wave vector.

The Heisenberg model has been studied using the Stochastic Series Expansion (SSE) QMC method<sup>17</sup>. The SSE method is also a finite-temperature QMC method based on the importance sampling of the diagonal matrix elements of the Taylor expansion of  $e^{-\beta H}$ . Ground state expectation values can be obtained by using sufficiently large values of  $\beta$ , and there are no approximations beyond statistical errors. With the recently developed “operator loop update”<sup>18</sup>, the method has proven to be very efficient tool for studying several different models.

In both approaches, we have measured the equal-time spin-spin correlation function  $\langle S_{\mathbf{i}} S_{\mathbf{j}} \rangle$  and the associated static spin structure factor in the momentum space given by

$$S(\mathbf{q}) = \frac{1}{N} \sum_{\mathbf{i}, \mathbf{j}} e^{\mathbf{q} \cdot (\mathbf{i} - \mathbf{j})} \langle (n_{\mathbf{i}, \uparrow} - n_{\mathbf{i}, \downarrow})(n_{\mathbf{j}, \uparrow} - n_{\mathbf{j}, \downarrow}) \rangle \quad (3)$$

We also evaluate the static spin susceptibility in the momentum space given by the Kubo integral

$$\chi(\mathbf{q}) = \int_0^\beta d\tau \langle S(-\mathbf{q}, \tau) S(\mathbf{q}, 0) \rangle \quad (4)$$

The magnon energy is calculated using the relation<sup>19</sup>

$$\omega(\mathbf{q}) = 2S(\mathbf{q})/\chi(\mathbf{q}). \quad (5)$$

We start the discussion of the numerical results by studying the convergence of the calculated quantities as a function of the inverse temperature,  $\beta$ . Figure 1 shows a plot of the magnon energies at the edge,  $(0, \pi)$ , and the center,  $(\pi/2, \pi/2)$ , of the zone boundary as a function of  $\beta$  for  $U = 6.0$ . The magnon energies are seen to converge to their  $T = 0$  values fairly rapidly with  $\beta$ . This convergence at relatively small values of  $\beta$  is not surprising given that we only deal with high-energy quantities. Henceforth, all the results presented are for  $\beta = 3.0$ .

Next we present the results for the magnon energies along the entire magnetic zone boundary for  $U =$

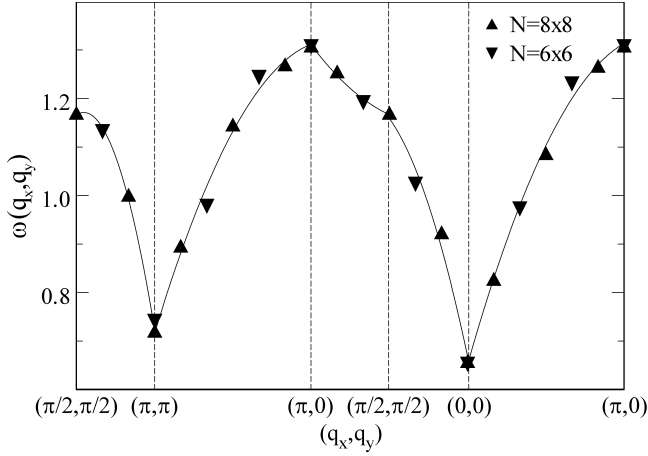


FIG. 2. The magnon dispersion along a path similar to Figure 3a in ref. 9 for 6x6 and 8x8 lattices at  $U = 6.0$  and  $\beta = 3.0$ . Error bars are smaller than symbol sizes.

6.0. This value of  $U$  is consistent with estimates of the effective on-site energy in  $\text{La}_2\text{CuO}_4$  obtained from photoemission<sup>20</sup> and optical<sup>21</sup> spectroscopy data. Figure 2 shows the variation of the magnon energy for a path along the Brillouin zone similar to the one considered in Figure 3a of ref. 9 for two different lattice sizes. Note that the data near  $(\pi, \pi)$  and  $(0, 0)$  are strongly temperature dependent, the latter being exactly proportional to temperature. However, as shown in Figure 1, the data along the zone boundary from  $(\pi, 0)$  to  $(\pi/2, \pi/2)$  have reached close to their zero temperature values. The qualitative nature of the variation of the magnon energy along the path is in good agreement with the experimental results and mean-field predictions. In particular, the magnon energy at the center of the zone boundary,  $(\pi/2, \pi/2)$ , is found to be lower than that at the edge,  $(0, \pi)$ , as seen in the experimental data and opposite to the dispersion found for the Heisenberg model. The magnitude of the deviation is estimated to be  $\approx -12\%$  of the  $N=8\times 8$  system, matching closely the experimental observation. While this quantitative agreement with experimental data is not conclusive—the magnon energies were evaluated in our calculation using the SMA, and the finite-size effects are fairly large—it is safe to conclude that the 2D Hubbard model, with a value of the on-site interaction energy in the range estimated from photoemission and optical spectroscopy data, can reproduce the correct magnon dispersion along the magnetic zone boundary.

We now discuss the variation of the dispersion along the zone boundary in the 2D Hubbard model as a function of the on-site interaction parameter,  $U$ . Figure 3 shows the results of our simulation for a  $N=8\times 8$  lattice at  $\beta = 3.0$ . We have focused primarily on the deviation of the magnon energy at the center of the zone boundary relative to the edges. To that end, we have scaled the magnon energies by their value at  $(0, \pi)$ . The deviation is seen to be maximum for the smallest value of  $U$  studied

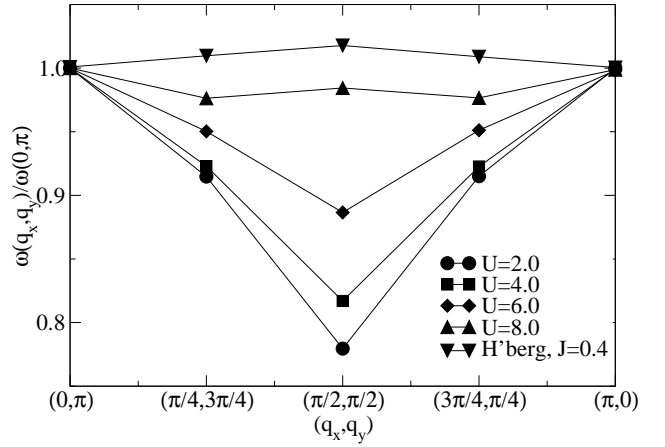


FIG. 3. Magnon dispersion along the magnetic zone boundary for different values of  $U$  for a  $N=8\times 8$  lattice at  $\beta = 3.0$ . The Heisenberg plot corresponds to  $U = 10.0$ . Error bars are of the order of symbol sizes.

and decreases with increasing  $U$ —becoming essentially flat within statistical error at  $U = 8.0$ . Unfortunately, for  $U > 8$ , the results of our simulation for the 2D Hubbard model become too noisy. However, in this limit of large  $U$ , the Hubbard model maps on to the Heisenberg model. Hence the dispersion for larger  $U$  values is expected to be qualitatively similar to that for the Heisenberg model. We have also shown in the figure the dispersion obtained for a Heisenberg model with exchange parameter  $J$  corresponding to  $U = 10.0$ . The point  $U = 8.0$  marks a transition to “Heisenberg-like” behavior. This value of the transition point is consistent with that found from specific heat measurements of the 2D Hubbard model<sup>22</sup>.

To investigate other possible sources for the nature of magnon energy dispersion along the magnetic zone boundary, we have studied the effects of spin-phonon coupling within the framework of the 2D Heisenberg model. The model involves coupling of the spins to dynamic optical bond phonons and is given by the Hamiltonian

$$H = -J \sum_{\langle \mathbf{i}, \mathbf{j} \rangle} (1 + \alpha(a_b^\dagger + a_b)) \mathbf{S}_i \cdot \mathbf{S}_j + \omega_0 \sum_b a_b^\dagger a_b \quad (6)$$

where  $b$  denotes the bond between the lattice sites  $\mathbf{i}$  and  $\mathbf{j}$  and the operator  $a_b^\dagger(a_b)$  creates(annihilates) a phonon on bond  $b$ .  $\omega_0$  represents the bare phonon frequency and  $\alpha$  measures the strength of the spin-phonon interaction.

The spin-phonon model was studied using the SSE QMC method. Our results indicate that over any reasonable range of spin-phonon coupling strength and bare phonon frequency, the magnon dispersion along the magnetic zone boundary is qualitatively the same as the pure Heisenberg model. Figure 4 shows the variation of the magnon energy along the same path in momentum space as considered in Figure 2 for the pure Heisenberg model and the spin-phonon model with  $\alpha = 0.1$  and  $\omega_0 = 0.25$  for a lattice of size  $N=8\times 8$  at  $\beta=5.0$ . The value of  $\beta$  is chosen such that  $\beta J$  is the same as  $\beta t$  for the data

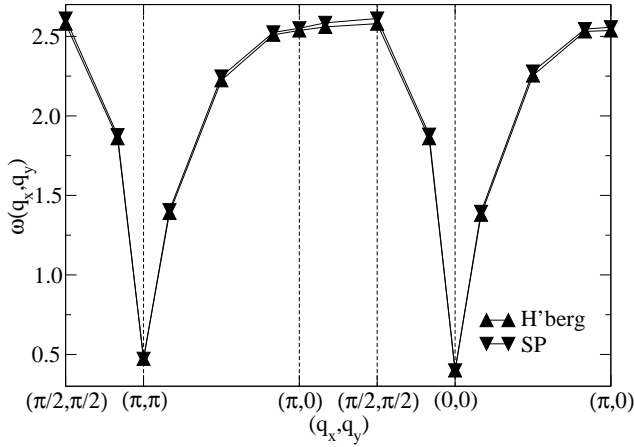


FIG. 4. Magnon dispersion along the same path as in Figure 2 for a  $N=8 \times 8$  lattice at  $\beta = 5.0$  for the pure Heisenberg model and the spin-phonon model with  $\alpha = 0.1$  and  $\omega_0 = 0.25$ .

presented in Figure 2 with  $J = 4t^2/U$ . This allows for a direct comparison between the two sets of data. Once again we found that while the data near  $(\pi, \pi)$  and  $(0, 0)$  are strongly temperature dependent, the magnon energies along the magnetic zone boundary from  $(\pi, 0)$  to  $(\pi/2, \pi/2)$  have converged close to their ground state values. The data suggests that the deviation in the magnon dispersion observed for  $\text{La}_2\text{CuO}_4$  from that found in the Heisenberg model cannot be explained by the type of spin-phonon coupling considered here. It remains to be seen whether a more realistic treatment of the electron-phonon coupling in the cuprates can account for this behavior.

To summarize, we have used the det QMC to show that the experimentally observed magnon dispersion along the magnetic zone boundary in  $\text{La}_2\text{CuO}_4$  can be reproduced by the 2D Hubbard model, using reasonable  $U/t$  values. The deviation of the magnon energy at the center of the zone boundary is maximum for the smallest value of  $U$  considered, where the charge fluctuations are the largest, and decreases with increasing  $U$ . For  $U \approx 8t$ , the dispersion is flat within statistical errors. The dispersion for larger values of  $U$  is qualitatively similar to that of the pure Heisenberg model. Thus, at  $U \approx 8t$ , there is a transition to “Heisenberg-like” behavior where the effects of the charge fluctuations become negligible. An interesting question is whether this intermediate  $U/t$  regime of the Hubbard model is equivalent to a Heisenberg plus ring exchange term. At really small  $U/t$  the electrons will be strongly delocalized, so that a description in terms of a spin Hamiltonian would break down. However, at the intermediate  $U/t$ , found in our calculations, a higher order perturbative treatment maybe justified leading to a Heisenberg plus ring exchange Hamiltonian.

We would like to thank Anders Sandvik for many useful discussions. This work was supported in part by NSF grant number 9986948. The numerical simulations were

carried out in part at the Condor Flocks at University of Wisconsin, Madison and NCSA, Urbana, Illinois.

- <sup>1</sup> S. Chakravarty, B. I. Halperin and D. R. Nelson, Phys. Rev. Lett. **60**, 1057 (1988); Phys. Rev. B **39**, 2344 (1989).
- <sup>2</sup> R. R. P. Singh and M. P. Gelfand, Phys. Rev. B **52**, 15695 (1995).
- <sup>3</sup> A. W. Sandvik and R. R. P. Singh, Phys. Rev. Lett. **86**, 528 (2001).
- <sup>4</sup> K. B. Lyons, P. E. Sulewski, P. A. Fleury, H. L. Carter, A. S. Cooper, G. P. Espinosa, Z. Fisk and S.-W. Cheong, Phys. Rev. B **39**, 9693 (1989); S. Sugai, M. Sato, T. Kobayashi, J. Akimitsu, T. Ito, H. Takagi, S. Uchida, S. Hosoya, T. Kajitani and T. Fukuda, *ibid.* **42**, 1045 (1990). R. R. P. Singh, P. A. Fleury, K. B. Lyons and P. E. Sulewski, Phys. Rev. Lett. **62**, 2736 (1989);
- <sup>5</sup> For a review of various optical studies see M. Gruninger in *Of spin and charge in the cuprates*, Ph. D. dissertation, University of Groningen, Netherlands.
- <sup>6</sup> B. S. Shastry and B. I. Shraiman, Phys. Rev. Lett. **65**, 1068 (1990).
- <sup>7</sup> D. Vaknin, S. K. Sinha, D. E. Moncton, D. C. Johnston, J. M. Newsam, C. R. Safinya and H. E. King, Jr., Phys. Rev. Lett. **58**, 2802 (1987); G. Shirane, Y. Endoh, R. J. Birgeneau, M. A. Kastner, Y. Hidaka, M. Oda, M. Suzuki and T. Murakami, *ibid.* **59**, 1613 (1987); G. Aeppli, S. M. Hayden, H. A. Mook, Z. Fisk, S.-W. Cheong, D. Rytz, J. P. Remeika, G. P. Espinosa and A. S. Cooper, *ibid.* **62**, 2052 (1989).
- <sup>8</sup> S. M. Hayden, G. Aeppli, R. Osborn, A. D. Taylor, T. G. Perring, S.-W. Cheong and Z. Fisk, Phys. Rev. Lett. **67**, 3622 (1991).
- <sup>9</sup> R. Coldea, S. M. Hayden, G. Aeppli, T. G. Perring, C. D. Frost, T. E. Mason, S.-W. Cheong and Z. Fisk, Phys. Rev. Lett. **86**, 5377 (2001).
- <sup>10</sup> H. M. Rønnow, D. F. McMorrow, R. Coldea, A. Harrison, I. D. Youngson, T. G. Perring, G. Aeppli, O. Syljuåsen, K. Lefmann and C. Rischel, Phys. Rev. Lett. **87**, 37202 (2001).
- <sup>11</sup> Y. J. Kim, A. Aharony, R. J. Birgeneau, F. C. Chou, O. Entin-Wohlman, R. W. Erwin, M. Greven, A. B. Harris, M. A. Kastner, I. Y. Korenblit, Y. S. Lee and G. Shirane, Phys. Rev. Lett. **83**, 852 (1999).
- <sup>12</sup> M. Takahashi, J. Phys. C **10**, 1289 (1977); A. H. MacDonald, S. M. Girvin and D. Yoshioka, Phys. Rev. B **37**, 9753 (1988); **41**, 2565 (1990).
- <sup>13</sup> M. Roger and J. M. Delrieu, Phys. Rev. B **39**, 2299 (1989).
- <sup>14</sup> A. Laeuchli and M. Troyer, unpublished; A. Sandvik and R. R. P. Singh, unpublished; A. A. Katanin and A. P. Kampf, cond-mat/0111533.
- <sup>15</sup> N. M. R. Peres and M. A. N. Araújo, cond-mat/0201151.
- <sup>16</sup> R. Blankenbecler, D. J. Scalapino, and R.L. Sugar, Phys. Rev. D **24**, 2278 (1981).
- <sup>17</sup> A. W. Sandvik and J. Kurkijärvi, Phys. Rev. B **43**, 5950 (1991); A. W. Sandvik, J. Phys. A **25**, 3667 (1992); A. W. Sandvik, Phys. Rev. B **56**, 11678 (1997).
- <sup>18</sup> A. W. Sandvik, Phys. Rev. B **59**, 14157 (1999).

- <sup>19</sup> A. W. Sandvik and A. Sudbø, *Europhys. Lett.* **36**, 443 (1996).
- <sup>20</sup> C. Kim, P. J. White, Z.-X. Shen, T. Tohyama, Y. Shibata, S. Maekawa, B. O. Wells, Y. J. Kim, R. J. Birgeneau, M. A. Kastner, *Phys. Rev. Lett.* **80**, 4245 (1998).
- <sup>21</sup> H.-B. Schüttler and A. J. Fedro, *Phys. Rev. B* **45**, 7588 (1992).
- <sup>22</sup> T. Paiva, R. T. Scalettar, C. Huscroft and A. K. McMahan, *Phys. Rev. B* **63**, 125116 (2001).